CHEMISTRY
AN ASIAN JOURNAL

DOI: 10.1002/asia.200900542

SnO_2@Poly(HEMA-*co*-St-*co*-VPBA) Core-shell Nanoparticles Designed for Selectively Enriching Glycopeptides Followed by MALDI-MS Analysis

Wen-Wen Shen,[a, b] Cheng-Ning Ma,[a] Su-Feng Wang,[a] Huan-Ming Xiong,*[a] Hao-Jie Lu,*[a, b] and Peng-Yuan Yang[a, b]

Abstract: The core-shell boronic-acid functionalized nanoparticles SnO_2@Poly(HEMA-*co*-St-*co*-VPBA) are designed for selectively enriching glycopeptides, followed by matrix-assisted laser desorption/ionization mass spectrometry (MALDI-MS) analysis. Such 60 nm sized core-shell nanoparticles are prepared by means of copolymerization between 2-hydroxyethyl methacrylate (HEMA) grafted on SnO_2 nanoparticles, styrene, and 4-vinylphenylboronic acid (VPBA). All of the synthesis procedures are completed within 3 h. Cyclic boronate esters form between boronic-acid groups on the polymer chains and *cis*-diol groups on glycopeptides, and thus almost all intact glycopeptides from low-abundant horseradish peroxidase (HRP) and bovine asialofetuin (ASF) are enriched with high selectivity and efficiency. After enrichment, both intact N- and O-glycopeptides are characterized by multistage MS. Furthermore, we successfully apply this method to the human serum sample for characterizing the target glycoproteins haptoglobin and alpha-1-acid-glycoprotein. The present selective enriching method followed by multistage-MS analysis is proven to be a good choice for routine glycopeptide characterization.

Keywords: core-shell nanoparticles · enrichment · glycopeptides · mass spectrometry · polymerization

Introduction

Protein glycosylation, as one of the most important post-translational modifications (PTMs), regulates cellular mechanisms, including cell adhesion, receptor activation, signal transduction, molecular trafficking and clearance, and endocytosis.[1] Many diseases are caused by glycosylation or glycosidase deficiencies, such as autoimmune disorders[2] or infantile-onset symptomatic epilepsy.[3] The US Food and Drug Administration has agreed that over half of the recent cancer biomarkers are glycoproteins.[4] To identify glycosylation sites, as well as the primary structures of the glycans, mass spectrometric strategies have been developed.[5] However, as glycopeptides are always low in abundance when the glycoprotein is digested into peptides,[6] the MS signals of nonglycosylated peptides always heavily interfere with those of glycopeptides. Moreover, determination of glycan structures is usually difficult because of their vast diversity.[1] Therefore, selective enriching methods followed by multistage MS techniques are necessary for glycopeptide analysis.

A lot of strategies have been developed for enriching glycopeptides. Among them, the methods based on physical properties of the glycopeptides, for example, size exclusion[7] and hydrophilic interaction chromatography,[8,9] are easily influenced by the complex components from practical samples. In contrast, the methods based on biospecificity or chemical binding have shown better performance on selective enriching. For example, lectin affinity chromatography is widely used for isolating glycopeptides from the peptide mixture based on the biospecificity interaction between lectin and the particular glycan structures.[10] However, this method is not suitable for the glycopeptides whose glycans cannot be recognized by the special lectin(s).[11] As another example, solid-phase micro-extraction through hydrazide chemistry depends on the covalent binding between the hydrazide resins and the oxidized *cis*-diol groups on gly-

[a] W.-W. Shen, C.-N. Ma, S.-F. Wang, Prof. Dr. H.-M. Xiong, Prof. Dr. H.-J. Lu, Prof. Dr. P.-Y. Yang
Department of Chemistry
Fudan University
220 Handan Road, Shanghai, 200433 (China)
Fax: (+86)21-54237961
E-mail: hmxiong@fudan.edu.cn
luhaojie@fudan.edu.cn

[b] W.-W. Shen, Prof. Dr. H.-J. Lu, Prof. Dr. P.-Y. Yang
Institutes of Biomedical Sciences
Fudan University
130 Dong′an Road, Shanghai, 200032 (China)

Supporting information for this article is available on the WWW under http://dx.doi.org/10.1002/asia.200900542.

cans.[12,13] Because this binding is irreversible, the following glycan cleavage by endoglycosidase, as required for MS analysis, always lost the glycan information. To obtain intact glycopeptides, it is optimal to utilize special chemical reactions to bond glycopeptides during enrichment and then recover them for analyses. Such reactions occur between polymers with oxylamino groups and aldehyde-attached glycopeptides,[14,15] or between boronic acid groups and 1,2-*cis*-diol on glycans.[16] The latter boronate chemistry method is gentle and easy to handle. Several boronic-acid functionalized materials have been reported to date, such as *m*-aminophenyl boronic-acid (APBA) functionalized agarose gels,[16,17] APBA magnetic microparticles,[18] APBA magnetic nanoparticles,[19] and APBA mesoporous silica.[20] These materials isolate samples by means of solid phase extraction except the functionalized agarose gels, which are always prepared as a stationary phase for affinity chromatography. In general, the procedures by solid phase extraction were easier to deal with.

In this study, we prepared SnO_2@Poly(HEMA-*co*-St-*co*-VPBA) core-shell nanoparticles with boronic-acid groups and successfully applied them in the enrichment of glycopeptides. These nanoparticles were synthesized by means of a hydroxyl-exchange reaction and a polymerization route. The products were uniform, stable, monodispersed in water and their diameters were only about 60 nm. They had large surface areas and plenty of boronic-acid groups, so that glycopeptides with *cis*-diol groups could be enriched with high selectivity and efficiency. After enrichment and recovery treatment, the obtained glycopeptides were analyzed by MALDI-MS for identifying glycosylation sites and the corresponding glycan structures.

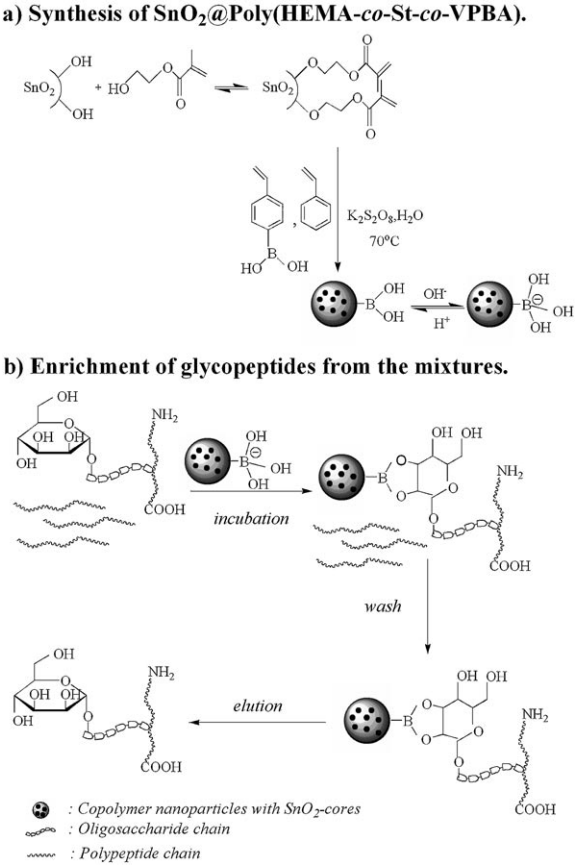

Scheme 1. a) Synthesis of SnO_2@Poly(HEMA-*co*-St-*co*-VPBA) nanoparticles and b) selective enrichment of glycopeptides using the nanoparticles.

Results and Discussion

Illustrated in Scheme 1 a are the synthetic routes of SnO_2@polymer nanoparticles. First, the freshly prepared SnO_2 nanoparticles were dispersed into 2-hydroxyethyl methacrylate (HEMA) to obtain the HEMA modified SnO_2. The exchange reaction mechanism has been reported in our previous work.[21,22] Secondly, the as-prepared SnO_2-HEMA sol was mixed with pure styrene (St) and 4-vinylphenylboronic acid (VPBA), and meanwhile, a solution containing styrene and $K_2S_2O_8$ was heated in water under stirring. After the two solutions were mixed together, copolymerization took place on the SnO_2-HEMA surfaces, resulting in nanoparticles with SnO_2-cores and hydrophilic boronic-acid surface groups. All of the procedures were completed within 3 h. It was rather simple and time-saving compared to the previous works, which needed over 16 h for the whole synthesis procedure.[18–20] The TEM images showed that the average diameter of the final produced uniform monodispersed nanoparticles was about 60 nm (Figure 1).

Abstract in Chinese:

摘要：本文根据硼酸根与顺式二羟基在不同 pH 条件下发生可逆化学反应的原理，设计合成出富含硼酸基团的纳米核壳材料，并发展了基于该材料并结合多级质谱分析的糖基化蛋白分析方法。该核壳材料约为 60 纳米直径大小，其核为二氧化锡纳米粒子，其壳是由嫁接在二氧化锡粒子表面的甲基丙烯酸羟乙酯, 苯乙烯和对乙烯基苯硼酸共聚而成。整个合成过程在 3 小时以内。研究表明，该核壳材料能够从糖基化蛋白中高效分离富集出完整的 N 型和 O 型糖肽，进而利用多级质谱对其富集到的糖肽进行糖链结构解析。该方法不仅适用于标准糖基化蛋白辣根过氧化物酶和脱唾液酸胎球蛋白，也适用于复杂体系中的糖基化蛋白。我们成功富集并解析了人类血清样本中的结合珠蛋白和酸性糖蛋白的糖肽。我们相信该富集分析方法有着良好的应用前景，可以成为糖蛋白分析的有效工具。

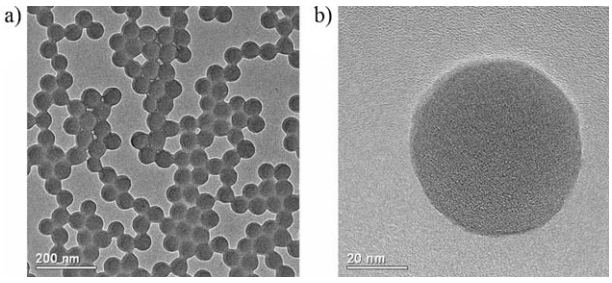

Figure 1. The TEM images of SnO_2@Poly(HEMA-*co*-St-*co*-VPBA) nanoparticles with different resolutions.

CHEMISTRY
AN ASIAN JOURNAL

The final produced nanoparticles were further characterized by IR, TGA, and ICP-AES measurements to investigate their structure and composition. IR spectra of SnO_2, SnO_2-HEMA, VPBA, and SnO_2@Poly(HEMA-*co*-St-*co*-VPBA) are shown in Figure S1 in the Supporting Information. The vibrations at $\tilde{\nu}=538$ and 661 cm^{-1} are ascribed to the Sn-O-Sn symmetric stretching inside SnO_2 nanoparticles and the Sn–O antisymmetric stretching on the SnO_2 surface, respectively.[22] Both vibrations are observed in the final nanoparticles, indicating that SnO_2 nanoparticles exist in the particle cores. The presence of HEMA in the final product is verified by the C=O stretching of ester groups at $\tilde{\nu}=$ 1717 cm^{-1}, whereas the presence of boronic-acid groups is verified by the B–O stretching at $\tilde{\nu}=1365$ and 1340 cm^{-1}.[23,24] Hence, the IR data confirms that the SnO_2 cores and boronic acid groups of the PHEMA related nanoparticle.

In Figure 2, thermogravimetric analysis (TGA) curves of SnO_2-HEMA and SnO_2@Poly(HEMA-*co*-St-*co*-VPBA) are shown. In Figure 2a, it is clear that there are three kinds of composition in the prepared SnO_2-HEMA sol. Physically adsorbed HEMA molecules (36.44 wt%) vaporized or decomposed before 150 °C, followed by the decomposition of the HEMA molecules that were chemically bounded to the SnO_2 surface (39.28 wt%). When the temperature rose above 400 °C, the reduction in weight stopped, indicating that only the inorganic component SnO_2 (24.28 wt%) remained. As for the SnO_2@Poly(HEMA-*co*-St-*co*-VPBA), four kinds of composition can be observed in Figure 2b. Between room temperature and 300 °C, small molecules from physical adsorption (6.61 wt%) vaporized or decomposed.

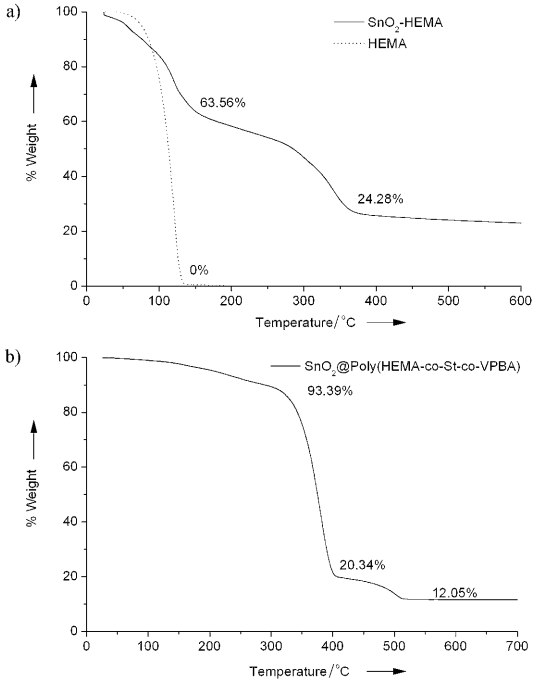

Figure 2. TGA curves of a) SnO_2-HEMA sols and HEMA, and b) SnO_2@Poly(HEMA-*co*-St-*co*-VPBA) nanoparticles.

Then, the polymers (73.05 wt%) decomposed within the range 300–400 °C, followed by decomposition of the remaining phenylboronic acid species (8.29 wt%). Finally, above 500 °C, SnO_2 and boron oxide remained (12.05 wt%). Analysis of the TGA data reveals that the content of B element is above 0.8 wt%. In addition, ICP-AES analysis indicated that there was 0.9 wt% B element in the nanoparticles. Thereby, the content of VPBA in the nanoparticles was calculated to be about 11 mg of VPBA segments in every 100 mg of powdered nanoparticles. For comparison, our previously reported APBA mesoporous silica contained 0.5 wt% B element.[20]

The affinity between the nanoparticle and glycopeptide was anticipated to be the typical boronate esterification since the boronic acid group could reversibly form cyclic-boronate esters with the 1,2-*cis*-diol of glycans,[16] as illustrated in Scheme 1b. To demonstrate that the newly prepared nanoparticles SnO_2@Poly(HEMA-*co*-St-*co*-VPBA) were able to selectively enrich glycopeptides from the mixture of glycosylated and non-glycosylated peptides, owing to the high contents of boronic-acid functional groups, mass spectra were acquired with both low and high mass ranges on the same spot by MALDI-MS. The final combined mass spectrum could have a wide range of mass from 500 to 6000 Da. In addition, SnO_2@Poly(HEMA-*co*-St) nanoparticles were used as a control material, to make sure that the enriching mechanism was based on the chemical reaction between VPBA of SnO_2@Poly(HEMA-*co*-St-*co*-VPBA) nanoparticles and glycopeptides. Two duplicate peptide mixtures of digested horseradish peroxidase (HRP) (1 mL and 100 ng mL^{-1}) were enriched by SnO_2@Poly(HEMA-*co*-St-*co*-VPBA) (Procedure I) or SnO_2@Poly(HEMA-*co*-St) (Procedure II). Both enriching procedures include exactly the same incubation–washing–elution sequence, as shown in Scheme 1b.

After the incubation step, no glycopeptides could be detected in the supernatant of Procedure I (Figure 3a), whereas many glycopeptide signals were found in the supernatant of Procedure II (Figure 3d), indicating that only the nanoparticles with boronic acid groups can selectively capture glycopeptides. After the washing step, the supernatant of Procedure I had only non-glycosylated peptides (Figure 3b), whereas the supernatant of Procedure II had both non-glycosylated peptides and glycopeptides (Figure 3e), indicating that non-glycosylated can interact with both nanoparticles through a non-specific manner. After the elution step, glycopeptides were expected to be released from the nanoparticles under the acidic condition if the adsorption interaction between the boronic-acid group and the *cis*-diol of glycans is specific. Indeed, glycopeptides were sensitively detected in the supernatant of Procedure I (Figure 3c), although no glycopeptides were seen in the supernatant of Procedure II (Figure 3f). Taking these results together, we can safely conclude that the interaction between the nanoparticles SnO_2@Poly(HEMA-*co*-St-*co*-VPBA) and glycopeptides is specific, arises from the boronic acid group on the surface of the nanoparticles.

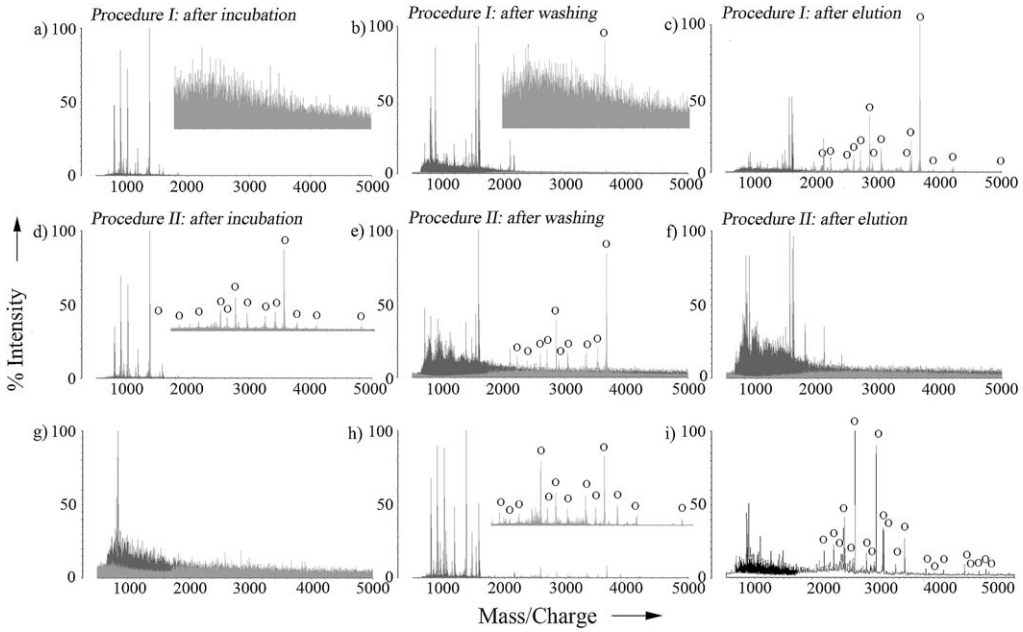

Figure 3. Mass spectra of digested proteins obtained by MALDI-MS. 100 ng mL^{-1} digested HRP treated by SnO_2@Poly(HEMA-*co*-St-*co*-VPBA) (Procedure I): a) the supernatant after incubation, b) the supernatant after washing and c) the supernatant after elution. 100 ng mL^{-1} digested HRP treated by SnO_2@Poly(HEMA-*co*-St) (Procedure II): d) the supernatant after incubation, e) the supernatant after washing and f) the supernatant after elution. g) 100 ng mL^{-1} digested HRP directly analyzed without enrichment. h) A total of 20 ng digested HRP. i) Glycopeptides enriched by SnO_2@Poly(HEMA-*co*-St-*co*-VPBA) from 1 μg mL^{-1} digested ASF. Each inset represents the magnified mass spectrum in the mass range of 2000–5000 Da. Peaks assigned to glycopeptides from HRP or ASF are marked by circles.

The enriching efficiency of the SnO_2@Poly(HEMA-*co*-St-*co*-VPBA) for glycopeptides was studied. No glycopeptide signal could be found by MS for 2 μL digested HRP with the concentration of 100 ng mL^{-1} without enriching procedure (Figure 3 g). After the enriching procedure, many signals assigned to glycopeptides were detected sensitively even 20% of the total eluent was analyzed (Figure 3 c). By contrast, 2 μL of digested HRP with the concentration of 10 μg mL^{-1} was analyzed and the mass spectrum is shown in Figure 3 h. In Figure 3 h, the signals of glycopeptides are suppressed in the presence of these nonglycopeptides, because the nonglycopeptides would compete in desorption/ionization with the glycopeptides. For instance, the ratios of signal-to-noise (S/N) of the three glycopeptide peaks in the enriched sample (*m*/*z*: 2851, 3672, 3527) were 687 (*m*/*z*: 2851), 244 (*m*/*z*: 3672), 137 (*m*/*z*: 3527), whereas the S/N of the same peaks for the sample with 100-fold higher concentration was 304, 141, and 77, respectively. Therefore, a S/N enhancement factor could be estimated for the two samples. As a result, the S/N enhancement factor for glycopeptides achieved was nearly 3 orders of magnitude.

The enriching capacity of the SnO_2@Poly(HEMA-*co*-St-*co*-VPBA) nanoparticles for glycopeptides was also studied here. The 1 mL aliquot of 10–150 ng mL^{-1} digested HRP was enriched by 100 ng nanoparticles. After enrichment, 10 μL elution solvent was added to release the glycopeptides and 0.5 μL eluent was spotted on the MALDI-plate for MS analysis. The glycopeptide (*m*/*z*: 3672) with the highest sensitivity here was used as the test peptide. If the concentration of the sample increased from 10 to 110 ng mL^{-1}, the S/N of this glycopeptide significantly increased. However, when the concentration increased over 110 ng mL^{-1}, the S/N of this glycopeptide stopped increasing, indicating that 100 ng nanoparticles reached enriching saturation for glycopeptides (Figure S2 in the Supporting Information). Therefore, we estimated the optimum enriching capacity of these nanoparticles for digested glycoprotein was about 1.1 g g^{-1} of glycopeptide. In addition, the glycopeptide at *m*/*z* 3672 was used for determination of the limit of detection (LOD) at a S/N of 3. As a result, LOD was calculated to be 0.5 ng mL^{-1}. By contrast, LOD of our most recent published material was about 2.5 ng mL^{-1}.[20]

To investigate the glycopeptides recovery of this enrichment method, the $^{18}O/^{16}O$ labeling method[25] was used here. Glycopeptides of another digested glycoprotein ASF (1 ng μL^{-1}) with both N-glycosylation sites and O-glycosylation sites were enriched by these nanoparticles from 1 mL solution and the mass spectrum is shown in Figure 3 i. Equal amounts of digested ASF without enrichment were used as a control. Then the two sample parts were processed by Poroszyme immobilized trypsin (bulk media, Applied Biosystems) and labeled with $H_2{}^{18}O/H_2{}^{16}O$ at the C-termini of the peptides from the enriched/control sample, respectively, as Wang et al. have previously described.[25] After $^{18}O/^{16}O$ labeling, the two parts were mixed and analyzed by MS. Two glycopeptides (*m*/*z* 3102 and *m*/*z* 2738) were used for calculation. With the equation described by Yao et al.[26] and the MS results (Figure S3 in the Supporting Information), the average recovery was calculated to be 86.1%.

This enrichment method followed by multistage MS analysis provided a solution for determining both glycosylation sites and glycan structures of glycopeptides. It is acknowledged that mainly 6 types of monosaccharides are composited of glycan chains and the glycan chains are linked on peptides by the regular rules.[5,7,27] Briefly speaking, there are mainly two types of glycopeptides, N- and O-glycopeptides. The N-glycopeptide requires the consensus sequence motif Asn-Xaa-Ser/Thr (Asn, asparagine; Ser, serine; Thr, threonine; Xaa is any amino acid except proline) and each glycan chain has a common core pentasaccharide $Man_3GlcNAc_2$ and extends in the form of bi-, tri-, or tetra-antennary structure. As for O-glycopeptide, glycosylation happens on the Ser/Thr residues, and the glycan chain has eight kinds of cores, which start with GalNAc (N-acetylgalactosamine). Under these rules, the potential glycosylation sites can be predicted from the identified protein sequence, and glycan structures can be predicted from the mass spectrum in the first stage because glycan fragmentation occurs prior to peptide fragmentation.[6] Then, the predictions of glycosylation sites and glycan structures are confirmed by multistage MS analysis. In this study, the intact glycopeptides from HRP and ASF were analyzed. From the mass spectra (Figures S4–S6 in the Supporting Information), their glycosylation sites and glycan structures were characterized. In agreement with other researchers,[28–30] the detected glycopeptides from HRP are N-glycopeptides and those from ASF are both N- and O-glycopeptides. Table 1 shows 5 detected N-glycosylation sites from HRP and 4 detected glycosylation sites from ASF. Among these, the two N-glycan structures from ASF were characterized as the tri-antennary form and the composition of its four glycosylation sites was determined by analysis of the mass spectra (Figures S5 and S6 in the Supporting Information). As for the intact O-glycopeptides of ASF, it was difficult to individually ascribe the specified saccharide residues, as the two predicted O-glycosylation sites were differentiated by only one amino acid residue. Nevertheless, this was the first time that multistage-MS has been used for preliminary description of intact O-glycopeptides in ASF.

Besides the standard samples, we then detected target glycoproteins in real biological sample by using this method. Our purpose was to characterize two of the important human serum glycoproteins, haptoglobin[31] and alpha-1-acid glycoprotein.[32] Because of the wide dynamic range of protein abundances in human serum, 6 μL human serum (about 60 $mg\,mL^{-1}$) was loaded on the Agilent Human 14 Multiple Affinity Removal System column for collecting high-abundant proteins and low-abundant proteins per the manufacturer's instruction, respectively. All of the low-abundant proteins and 10% of the high-abundant proteins were separated by sodium dodecyl sulfate/polyacrylamide gel (SDS-PAGE) electrophoresis (Figure 4). After separation, peptides were extracted from the protein bands in the high-abundant proteins lane and divided into 10 units for storage. 1-unit peptide solution from each band was used for protein identification per the previously reported method.[33] The protein results are displayed in Table S1 in the Supporting Information. After that, another 1-unit peptide solution of alpha-1-acid glycoprotein and haptoglobin (detected as No. 5 and 6 in Figure 4) was processed by SnO_2@Poly(HEMA-*co*-St-*co*-VPBA) nanoparticles. Validated by the other report,[34] glycopeptides with 4 N-glycosylation sites in both haptoglobin and alpha-1-acid glycoproteins were isolated and detected from the mass spectra (Figures S7 and S8 in the Supporting Information), as shown in Table 1. To our best knowledge, there are few studies on characterization of intact glycopeptides from real biological samples by using multistage-MS. Our method based on SnO_2@Poly(HEMA-*co*-St-*co*-VPBA) nanoparticles might be widely applied in the future for detecting target glycopeptides.

Table 1. List of the MS detected glycopeptides with their glycans at the glycosylation sites.

Peptide sequence with glycosylation site(s)[a]	Glycan composition[b]
Standard HRP	
QLTPTFYD#N_{43}SC(AAVESACPR)PNVSNIVR[c]	(GlcNAc)2(Man)3(Fuc)1(Xyl)1
LHFHDCFVNGCDASILLD#N_{87}TTSFR	(GlcNAc)2(Man)3(Fuc)1(Xyl)1
PTL#N_{228}TTYLQTLR	(GlcNAc)2(Man)3(Fuc)1(Xyl)1
LY#N_{216}FSNTGLPDPTL#N_{228}TTYLQTLR	(GlcNAc)4(Man)6(Fuc)2(Xyl)2
GLIQSDQELFSSP#N_{285}ATDTIPLVR	(GlcNAc)2(Man)3(Fuc)1(Xyl)1
Standard ASF	
PTPLA#N_{99}C*SVR[d]	(GlcNAc)5(Man)3(Gal)3
VVHAVEVALATFNAES#N_{176}GSYLQLVEISR	(GlcNAc)5(Man)3(Gal)3
AAGP#T_{280}P#S_{282}AAGPPVASVVVGPSVVAVPLPLHR	(HexNAc)6(Hex)6
Haptoglobin from human serum	
MVSHH# N_{184}LTTGATGATLINEQWLLTTAK	(GlcNAc)5(Man)5(Gal)2(Fuc)1
NLFL#N_{207}HSE#N_{211}ATAK	(GlcNAc)7(Man)6(Gal)3
VVLHP #N_{241}YSQVDIGLIK	(GlcNAc)4(Man)3(Gal)2
Alpha-1-acid glycoprotein from human serum	
QIPLCA#NLVPVPIT#N_{33}ATLDQITGK	(GlcNAc)2(Man)2(Fuc)1
NEEY#N_{56}K	(GlcNAc)6(Man)3(Gal)3(Fuc)1
QCIY#N_{93}TTYLNVQR	(GlcNAc)4(Man)3(Gal)1
E#N_{103}GTISR	(GlcNAc)3(Man)3(Gal)1

[a] Glycosylation sites are marked on the peptide sequence with a hash sign. [b] GlcNAc, N-acetylglucosamine; HexNAc, N-acetylglucosamine or N-acetylgalactosamine; Man, mannose; Gal, galactose; Hex, mannose or galactose; Fuc, fucose; Xyl, xylose. [c] Two cysteine are linked by a disulfide bond. [d] Asterisk represents cysteine carboxymethylation by IAA.

Conclusions

In summary, we have synthesized SnO_2@Poly(HEMA-*co*-St-*co*-VPBA) core-shell nanoparticles for selectively enriching glycopeptides from the peptide mixtures, and developed a time-saving procedure to recover the

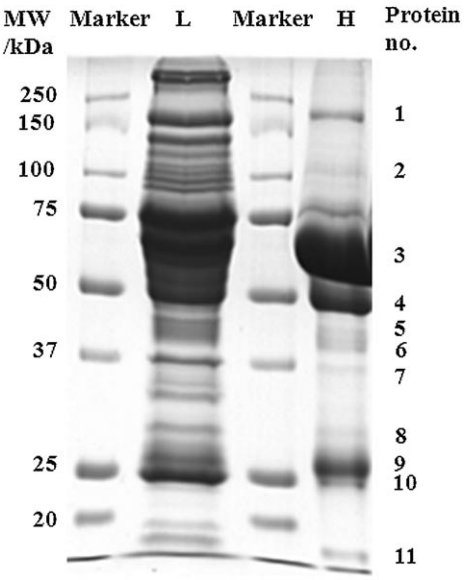

Figure 4. 1-DE map (10% SDS-PAGE) of high-abundant proteins and low-abundant proteins isolated from human serum. 'L' represents low-abundant proteins obtained from 6 μL serum; 'H' represents high-abundant proteins obtained from 0.6 μL serum. After the electrophoresis separation, the gels were stained by Coomassie brilliant blue. Arabic numerals designate lanes assigned to the proteins shown in Table S1 in the Supporting Information. Glycopeptides from No. 5 and 6 in 'H' were enriched by SnO_2@Poly(HEMA-*co*-St-*co*-VPBA) nanoparticles.

glycopeptides for MS analysis. The enrichment mechanisms are based on the reversible boronate esterfication between the nanoparticle boronic surface groups and 1,2-*cis*-diol from glycopeptides, and thus, glycopeptides are recovered with high selectivity and efficiency. Simultaneous identification of the glycosylation site and glycan structure can be achieved by mass spectrometric analysis of the enriched intact glycopeptide from both standard and real biological samples.

Experimental Section

Synthesis of SnO_2@Poly(HEMA-co-St-co-VPBA) Nanoparticles

The freshly prepared SnO_2 nanoparticles, which were obtained by hydrolyzing a 0.5 M $SnCl_4$ aqueous solution in a poly(tetrafluoroethylene) (PTFE)-lined autoclave at 160 °C for 2 h, were centrifuged, and then the white precipitates were dispersed in liquid 2-hydroxyethyl methacrylate (HEMA, Acros Organics) monomers. The solutions were precipitated and washed by absolute ether as a nonsolvent. The product was designated as SnO_2-HEMA in which HEMA groups were connected to the SnO_2 nanoparticles through covalent bonds. The freshly prepared SnO_2-HEMA were re-dispersed in styrene (St) and then mixed with the 4-vinylphenylboronic acid (VPBA, Johnson Matthey). In the beginning, St (2 g) and Milli-Q water (30 mL) were mixed and heated with stirring under nitrogen atmosphere. When the temperature rose to 70 °C, $K_2S_2O_8$ initiator (0.1 g) was added. After 5 min, St (2 g) containing SnO_2-HEMA and VPBA was injected into the reaction system. The weight ratio of total styrene to VPBA was 40:1. The copolymerization was performed at 70 °C for 1 h to obtain a milky suspension. After cooling to room temperature, the product was washed by chloroform and then centrifuged at 16000 rpm for 30 min to remove the supernatant. The precipitated gel-like beads could be re-dispersed in Milli-Q water by sonication. In this way, they could be purified by washing/centrifugation repeatedly. The beads were designated as SnO_2@Poly(HEMA-*co*-St-*co*-VPBA) with the core-shell structure. For comparison, the SnO_2@Poly(HEMA-*co*-St) nanoparticles were prepared under the same conditions excluding VBPA.

Characterization

The suspensions of SnO_2@copolymer core-shell nanoparticles were dropped onto small copper meshes to obtain TEM images by using a JEM-2010 transmission electron microscope operated at 200 kV. The nanoparticles were dropped on KBr pellets and dried under vacuum at 100 °C to prepare samples for infrared measurements by using a Nicolet Nexus 470 FTIR spectrometer. The dried nanoparticles were analyzed by thermogravimetric analysis (TGA) by using a Perkin–Elmer TGA 7 thermal analyzer in nitrogen with a heating rate of 10 °C min^{-1}. The contents of B element in the nanoparticles were determined by using an inductively coupled plasma atomic emission spectrometry (ICP-AES) by using a Hitachi P-4010 instrument operated at 40.68 MHz.

Enrichment of Glycopeptides

For standard proteins, an aliquot of SnO_2-copolymer nanoparticles suspension (1 μL, 0.1 mg mL^{-1}) was added into NH_4HCO_3 aqueous solution (1 mL, 50 mM, pH 8) containing a certain concentration of digested horseradish peroxidase (HRP, 100 ng mL^{-1}; Sigma), or bovine asialofetuin (ASF, 1 μg mL^{-1}; Sigma). ASF was reduced by dithiothreitol (DTT) and alkylated by iodoacetamide (IAA) before it was digested by trypsin (Sigma). For the real samples from human serum, each of the 1-unit peptide solution was lyophilized and then diluted by NH_4HCO_3 aqueous solution (0.3 mL, 50 mM, pH 8), followed by adding a 1 μL aliquot of SnO_2-copolymer nanoparticles suspension (0.1 mg mL^{-1}). This solution was then incubated for 2 h with vortexing at room temperature and then centrifugated at 16000 rpm for 20 min. After the supernatant was decanted, the deposit was washed repeatedly by NH_4HCO_3 aqueous solution. Then acidic aqueous solution (10 μL) containing 1% trifluoroacetic acid (TFA) was added into the washed deposit to release the glycopeptides from the nanoparticles for 1 h. In addition, the supernatant from centrifugation after incubation or washing was concentrated and re-dispersed by acidic aqueous solution (10 μL) containing 1% TFA.

MALDI MS Analysis

For standard proteins, every 2 μL of eluate or concentrated supernatant was dried on the MALDI plate. For the real samples from human serum, all the eluate from each sample was spotted. Then each of them was mixed with the matrix (1 μL, 10 mg mL^{-1} 2,5-dihydroxy benzoic acid dissolved in 50% (v/v) acetonitrile/water solution containing 0.1% TFA; Sigma) for MS analysis. All mass spectra were acquired by using a MALDI-Quadrupole Ion Trap-TOF mass spectrometer (AXIMA QIT, Shimadzu). MALDI was completed by utilizing a nitrogen pulsed laser (337 nm, 3–5 ns full width half maximum peak-width, FWHM). For collision-induced dissociation, argon was used as the collision gas. External mass calibration was performed by using fullerite clusters. Two kinds of ion trapping modes were chosen here: the mid-mass range (masses above 750 Da) and the higher-mass range (masses above 2 000 Da). All spectra were taken from the signal average of 100 profiles. The laser intensity was kept constant.

Acknowledgements

This study was supported by the National Science and Technology Key Project of China (2007CB914100, 2008ZX10207, 2009CB825607, and 2006AA02A308), the National Natural Science Foundation of China (20735005, 20875016, 30672394, and 20873029), the Ph.D. Programs Foundation of the Ministry of Education of China (200802460011), NCET, and Shanghai Projects (08DZ2293601, Shu Guang, Eastern Scholar, 09QA1400400 and B109).

[1] K. Ohtsubo, J. D. Marth, *Cell* **2006**, *126*, 855–867.
[2] R. L. Easton, M. S. Patankar, G. F. Clark, H. R. Morris, A. Dell, *J. Biol. Chem.* **2000**, *275*, 21928–21938.
[3] M. A. Simpson, H. Cross, C. Proukakis, D. A. Priestman, D. C. Neville, G. Reinkensmeier, H. Wang, M. Wiznitzer, K. Gurtz, A. Verganelaki, *Nat. Genet.* **2004**, *36*, 1225–1229.
[4] J. A. Ludwig, J. N. Weinstein, *Nat. Rev. Cancer* **2005**, *5*, 845–856.
[5] A. Dell, H. R. Morris, *Science* **2001**, *291*, 2351–2356.
[6] B. A. Budnik, R. S. Lee, J. A. J. Steen, *Biochim. Biophys. Acta Proteins Proteomics* **2006**, *1764*, 1870–1880.
[7] G. Alvarez-Manilla, J. Atwood, III, Y. Guo, N. L. Warren, R. Orlando, M. Pierce, *J. Proteome Res.* **2006**, *5*, 701–708.
[8] Y. Wada, M. Tajiri, S. Yoshida, *Anal. Chem.* **2004**, *76*, 6560–6565.
[9] M. Tajiri, S. Yoshida, Y. Wada, *Glycobiology* **2005**, *15*, 1332–1340.
[10] H. Kaji, H. Saito, Y. Yamachi, T. Shinkawa, M. Taoka, J. Hirabayashi, K. Kasai, N. Takahashi, T. Isobe, *Nat. Biotechnol.* **2003**, *21*, 667–672.
[11] R. Q. Qiu, F. E. Regnier, *Anal. Chem.* **2005**, *77*, 2802–2809.
[12] H. Zhang, X. J. Li, D. B. Martin, R. Aebersold, *Nat. Biotechnol.* **2003**, *21*, 660–666.
[13] B. Y. Sun, J. A. Ranish, A. G. Utleg, J. T. White, X. W. Yan, B. Y. Lin, L. Hood, *Mol. Cell. Proteomics* **2007**, *6*, 141–149.
[14] M. Kurogochi, M. Amano, M. Fumoto, A. Takimoto, H. Kondo, S. I. Nishimura, *Angew. Chem.* **2007**, *119*, 8964–8969; *Angew. Chem. Int. Ed.* **2007**, *46*, 8808–8813.
[15] N. Nagahori, M. Abe, S. I Nishimura, *Biochemistry* **2009**, *48*, 583–594.
[16] Q. B. Zhang, A. A. Schepmoes, J. W. C. Brock, S. Wu, R. J. Moore, S. O. Purvine, J. W. Baynes, R. D. Smith, T. O. Metz, *Anal. Chem.* **2008**, *80*, 9822–9829.
[17] B. J. Gould, P. M. Hall, *Clin. Chim. Acta* **1987**, *163*, 225–230.
[18] K. Sparbier, T. Wenzel, M. Kostrzewa, *J. Chromatogr. B* **2006**, *840*, 29–36.
[19] W. Zhou, N. Yao, G. P. Yao, C. H. Deng, X. M. Zhang, P. Y. Yang, *Chem. Commun.* **2008**, 5577–5579.
[20] Y. W. Xu, Z. X. Wu, L. J. Zhang, H. J. Lu, P. Y. Yang, P. A. Webley, D. Y. Zhao, *Anal. Chem.* **2009**, *81*, 503–508.
[21] H. M. Xiong, X. Y. Guan, L. H. Jin, W. W. Shen, H. J. Lu, Y. Y. Xia, *Angew. Chem.* **2008**, *120*, 4272; *Angew. Chem. Int. Ed.* **2008**, *47*, 4204–4207.
[22] H. M. Xiong, W. Z. Shen, Z. D. Wang, X. Zhang, Y. Y. Xia, *Chem. Mater.* **2006**, *18*, 3850–3854.
[23] K. F. Voss, C. M. Foster, L. Smilowitz, D. Mihailovic, S. Askari, G. Srdanov, *Phys. Rev. B* **1991**, *43*, 5109–5118.
[24] T. Ishi-i, K. Nakashima, S. Shinkai, *Tetrahedron* **1998**, *54*, 8679–8686.
[25] J. S. Wang, P. Gutierrez, N. Edwards, C. Fenselau, *J. Proteome Res.* **2007**, *6*, 4601–4607.
[26] X. D. Yao, A. Freas, J. Ramirez, P. A. Demirev, C. Fenselau, *Anal. Chem.* **2001**, *73*, 2836–2842.
[27] D. S. Dalpathado, H. Desaire, *Analyst* **2008**, *133*, 731–738.
[28] M. Wuhrer, C. H. Hokke, A. M. Deelder, *Rapid Commun. Mass Spectrom.* **2004**, *18*, 1741–1748.
[29] Y. Yang, R. Orlando, *Rapid Commun. Mass Spectrom.* **1996**, *10*, 932–936.
[30] M. G. Yet, C. Q. Chin, F. Wold, *J. Biol. Chem.* **1988**, *263*, 111–117.
[31] F. Yang, J. L. Brune, W. D. Baldwin, D. R. Barnett, B. H. Bowman, *Proc. Natl. Acad. Sci. USA* **1983**, *80*, 5875–5879.
[32] L. Dente, M. G. Pizza, A. Metspalu, R. Cortese, *EMBO J.* **1987**, *6*, 2289–2296.
[33] W. W. Shen, H. M. Xiong, Y. Xu, S. J. Cai, H. J. Lu, P. Y. Yang, *Anal. Chem.* **2008**, *80*, 6758–6763.
[34] T. Liu, W. J. Qian, M. A. Gritsenko, D. G. Camp II, M. E. Monroe, *J. Proteome Res.* **2005**, *4*, 2070–2080.

Received: October 10, 2009
Revised: December 31, 2009
Published online: March 16, 2010

